**Correspondence to:**
D. J. Raymond,
raymond@kestrel.nmt.edu

# Predicting convective rainfall over tropical oceans from environmental conditions

**David J. Raymond[1] and Marcos M. Flores[1]**

[1]Physics Department and Geophysical Research Center, New Mexico Tech, Socorro, New Mexico, USA

**Abstract** A cloud resolving model in spectral weak temperature gradient mode is used to explore systematically the response of mean convective rainfall to variations tropical environmental conditions. A very large fraction of the variance in modeled rainfall is explained by three variables, the surface moist entropy flux, the instability index (a measure of low to midlevel moist convective instability), and the saturation fraction (a kind of column-averaged relative humidity). The results of these calculations are compared with the inferred rainfall from 37 case studies of convection over the tropical west Pacific, the tropical Atlantic, and the Caribbean, as well as in the NCEP FNL analysis and the ERA-Interim reanalysis. The model shows significant predictive skill in all of these cases. However, it consistently overpredicts precipitation by about a factor of three, due possibly to simplifications made in the model. These calculations also show that the saturation fraction is not a predictor of rainfall in the case of strong convection. Instead, saturation fraction covaries with the precipitation as a result of a moisture quasi-equilibrium process.

## 1. Introduction

Prediction of convective rainfall is one of the most important functions of cumulus parameterizations in large-scale numerical models. The problem with many cumulus parameterizations is that their performance is difficult to untangle from other effects in a large-scale model. However, this situation is changing with the employment of various cloud-resolving numerical modeling techniques. Such models are not the real world, but results from super parameterization schemes, in which a small cloud model is run in each large-scale grid box, are often better than conventional cumulus parameterizations in their predictions, indicating that they have something to teach us [*Khairoutdinov et al.*, 2005, 2008].

Cumulus parameterizations are generally constrained to use only current, resolved-scale conditions available from the encompassing large-scale model. These potentially include surface fluxes of heat, moisture, and momentum, sea surface temperature (over oceans), radiative forcing, and the vertical profiles of temperature, humidity, and wind.

Treatments of cumulus convection have traditionally been deterministic, in that the behavior of the convection is completely specified by the resolved-scale conditions. However, there is increasing interest in incorporating random fluctuations in parameterizations so as to reproduce the observed variability of convection and precipitation [*Palmer*, 2001; *Lin and Neelin*, 2000, 2003; *Plant and Craig*, 2008; *Khouider et al.*, 2010; *Groenemeijer and Craig*, 2012; *Peters et al.*, 2013; *Dorrestijn et al.*, 2015].

Nondeterminate fluctuations in convection and rainfall are an important part of the cumulus parameterization problem. However, our goal in this paper is to understand the determinate part of these phenomena, as this forms the mean state about which fluctuations take place.

There is a temptation to use gradient quantities such as mass and moisture convergence to drive cumulus parameterizations in models. However, this is likely to be problematic, as these convergence-related variables are at least partly a result of the convection itself rather than a cause [see e.g., *Raymond and Emanuel*, 1993], at least in the tropics where quasi-geostrophic forcing is minimal. Even in middle latitudes the total convergence is the sum of the large-scale balanced contribution (mostly quasi-geostrophic or boundary layer in origin) and convergence induced by the convection itself. Models such as wave-CISK (convective instability of the second kind), e.g., *Lindzen* [1974] that drive parameterized convection with gradient quantities like mass or moisture convergence, often exhibit an "ultraviolet catastrophe" in which instability growth rates asymptote to infinity for large wavenumbers. *Ooyama* [1982] characterizes these as aliased

models of convective instability of the first kind in disguise. We therefore hypothesize that the average state of convection, and the precipitation in particular, is a function only of nongradient environmental variables.

*Ooyama* [1982] further asserted that convection can only be parameterized in terms of the balanced part of the environmental flow. This part of the flow is derived from the potential vorticity distribution and generally has an evolution time scale longer than that of the convection itself, indicating that the arrow of causality points from the balanced flow to the convection. The unbalanced part of the flow is related in an intimate and complex manner to the convection itself and it is impossible to say that one causes the other—they coevolve. This coevolution and the fact that the convection is turbulent means that the unbalanced part of the flow (including the convection) has a chaotic component. Only the statistical behavior of the convection can be predicted and this prediction must come from the balanced part of the environmental flow.

The particular mechanism of convective control of most interest to *Ooyama* [1982] was the "cooperative intensification mechanism" that occurs in the core of tropical storms. In this mechanism boundary layer frictional convergence drives convection, which in turn increases the boundary layer circulation via the hydrostatic decrease in surface pressure due to convective warming aloft. This only acts reliably when the vorticity is strong enough to make the Rossby radius comparable to the spatial scale of a convective cell. In less extreme situations, the balanced flow may still control the statistical characteristics of the convection, but the mechanism is likely to be different. As *Ooyama* [1982] points out, frictional convergence may still exist in this case, but it is typically less effective than other mechanisms, e.g., surface heat and moisture fluxes, in destabilizing the atmosphere to moist convection.

*Raymond et al.* [2015] proposed a model for the interaction between convection and balanced circulations that are not strong enough to activate Ooyama's cooperative intensification mechanism. In this "thermodynamic" regime, which covers many if not most tropical disturbances, convection is hypothesized to be forced primarily by thermodynamic effects. A key diagnostic in this case is the gross moist stability. A particular version of this variable called the normalized gross moist stability was defined by *Raymond and Sessions* [2007] and expanded upon by *Raymond et al.* [2009]. In the steady state, this quantity becomes

$$\Gamma = \frac{T_R(F_s - R)}{L(P - E)} \qquad (1)$$

where $F_s$ is the surface moist entropy flux, $E$ is the surface evaporation rate, $R$ is the radiative sink of entropy integrated over the troposphere, and $P$ is the precipitation rate. Normalizing constants are a reference temperature $T_R$ and the latent heat of condensation $L$. Solving this for the net precipitation rate (precipitation minus evaporation) yields

$$P - E = \frac{T_R(F_s - R)}{L\Gamma}. \qquad (2)$$

For (2) to be useful, a model is needed for the the normalized gross moist stability. This comes from the realization that in a steady state $F_s - R$ equals the vertically integrated lateral detrainment of moist entropy. (The irreversible generation of entropy is assumed to be negligible here, but can be added to the analysis if needed.) This detrainment rate is a function of the structure and areal density of convection; the smaller this detrainment rate for a single convective cell, the larger is the number of cells per unit area needed to balance the steady state entropy budget.

Assuming positive $\Gamma$, the net precipitation rate is only positive when the surface entropy flux exceeds the radiative loss of entropy from the troposphere. Thus, strong surface entropy flux is a prerequisite for intense mean precipitation in this model. Furthermore, the effects of the surface entropy flux are amplified by low values of the gross moist stability. Observations, theory, and modeling have shown that the surface moist entropy flux exerts strong control over the amount of deep convection and mean rainfall rates [*Ooyama*, 1969; *Emanuel*, 1986, 1987; *Yano and Emanuel*, 1991; *Raymond*, 1995; *Raymond et al.*, 2003; *Maloney and Sobel*, 2004; *Back and Bretherton*, 2005; *Raymond and Zeng*, 2005; *Raymond et al.*, 2006; *Raymond and Sessions*, 2007; *Sobel et al.*, 2009; *Wang and Sobel*, 2011, 2012]. This dependence is important for the development of both tropical cyclones and intraseasonal oscillations.

Observations also show that small changes in the vertical profiles of temperature and humidity have dramatic effects on the gross moist stability and hence the rainfall rate over tropical oceans [*Raymond et al.*, 2011;

*Komaromi*, 2013; *Gjorgjievska and Raymond*, 2014; *Sentić et al.*, 2015]. In particular, increased saturation fraction (a kind of column-averaged relative humidity) and decreased low to midlevel moist convective instability (characterized by the instability index) are associated with an increase in the mean convective precipitation rate in developing tropical storms. In addition, decreased instability is related to an increase in convective mass fluxes at low levels and a decrease aloft, i.e., it makes these mass fluxes more bottom-heavy. Both of these effects act by decreasing the gross moist stability, as illustrated by (2). Basically, this occurs by increasing the vertically integrated moisture convergence, which increases precipitation in the steady state.

Weak temperature gradient (WTG) convective simulations [*Sobel and Bretherton*, 2000; *Raymond and Zeng*, 2005; *Raymond and Sessions*, 2007; *Wang et al.*, 2013; *Herman and Raymond*, 2014; *Sessions et al.*, 2015; *Sentić et al.*, 2015] are in agreement with these observations, suggesting that this modeling technique is a useful tool in understanding deep convection over tropical oceans.

This paper reports on a systematic exploration of the sensitivity of time and space averaged precipitation to variations in environmental conditions in convection simulated using a WTG convective model. By taking an average, we exclude the chaotic variations in convection resulting from small-scale turbulent dynamics and concentrate on those properties of convection constrained by balanced dynamics and thermodynamic conservation laws. Thus, comparison of model precipitation with real world values requires a large degree of smoothing of observations.

An important aspect of any convective modeling exercise is determining how to relate model results to the real world. This is particularly tricky when questions of causality arise. For instance, are the surface moist entropy fluxes, the instability index, and the saturation fraction imposed by the environment or are they artifacts of the convection itself? Considerable effort is addressed to this issue here.

This investigation is preliminary in that certain simplifying assumptions are made, to be discussed later in the paper. The results are nevertheless interesting in that the model for precipitation rate resulting from these simulations exhibits significant skill in reproducing actual mean precipitation rates via mechanisms observed in the real world.

The experimental design of the study is reported in section 2 and the results of the modeling are presented in section 3. A comparison with observations is given in section 4 and conclusions are presented and discussed in section 5.

## 2. Experiment Design

The spectral weak temperature gradient (SWTG) model [*Herman and Raymond*, 2014] is used in two-dimensional mode with fixed radiation and sea surface temperature (SST). A radiative-convective equilibrium calculation is first made to provide a base state about which perturbations in temperature and humidity profiles, sea surface temperature, and imposed wind speed are made to produce a wide variety of reference profiles and surface conditions for the weak temperature gradient calculations. The results are then categorized according to surface moist entropy flux, the instability index, and the saturation fraction. These parameters have been shown to be important for precipitation production [*Gjorgjievska and Raymond*, 2014]. The instability index II is defined

$$II = s_{lo}^* - s_{hi}^*, \tag{3}$$

where $s_{lo}^*$ is the saturated moist entropy averaged over the range $[1, 3]$ km and $s_{hi}^*$ is this quantity averaged over $[5, 7]$ km. It is a measure of low to midtroposphere moist convective instability. The saturation fraction SF is

$$SF = \int r\, dp \bigg/ \int r^*\, dp \tag{4}$$

where $r$ is the mixing ratio and $r^*$ is the saturation mixing ratio. It is a kind of column-averaged relative humidity.

### 2.1. SWTG Model

WTG convective simulations relax the areally averaged convective domain profile of potential temperature in a cloud resolving model to a reference profile that is deemed to represent the environment surrounding the convection. This relaxation is assumed to be the result of gravity wave action that distributes buoyancy anomalies over a large area [*Bretherton and Smolarkiewicz*, 1989]. The time scale $\tau$ for the relaxation is taken to be that of the gravity waves. A flaw in traditional WTG calculations is that gravity waves of all vertical scales are assumed to propagate at the same speed. In the real world, gravity waves of different vertical scales move at different speeds, resulting in multiple time scales.

In the SWTG model, the buoyancy anomaly in the convective domain (i.e., the difference between the convective domain and reference profile potential temperatures) is subjected to a Fourier decomposition in the vertical. Each Fourier mode with a given vertical wavenumber $m_j = j\pi/h$ is assigned a relaxation time proportional to this wavenumber

$$\tau_j = L m_j / N = j\pi L/(hN) \quad j = 1, 2, 3, \ldots \tag{5}$$

where $h$ is the depth of the troposphere, $N$ is the tropospheric Brunt-Väisälä frequency (assumed constant with height), and $L$ is an assumed horizontal length scale. Thus, shallower modes relax more slowly to the reference profile than deeper ones in agreement with the dynamics of hydrostatic gravity waves. This spectral decomposition yields a more physically realistic relaxation process than is obtained by assuming that all vertical scales relax at the same rate, as is done in classical WTG. The length scale $L$ is assumed to be the distance traveled by a $j = 1$ gravity wave over the convective life cycle time of order 1 hr. We take $L = 150$ km in the present work.

Precipitating convection differs from other forms of convection in that the subsiding branch of the circulation has a much larger scale than the ascending branch. The SWTG vertical velocity is assumed to represent the ascending branch of the convective circulation. It is given by

$$w_{swtg}(z) = \sum_j \frac{\Theta_j}{\tau_j} \sin(m_j z) \tag{6}$$

where

$$\Theta_j = \frac{2}{h} \int_0^h \frac{\theta'(z) \sin(m_j z)}{d\bar{\theta}/dz} dz. \tag{7}$$

The quantity $\theta'(z)$ is the potential temperature anomaly, defined as the horizontal mean of potential temperature in the convective domain $\bar{\theta}(z)$ minus the reference profile $\theta_R(z)$, and $\Theta_j$ is the projection of $\theta'/(d\bar{\theta}/dz)$ onto the $j$th spectral mode.

Moisture and moist entropy are given horizontally uniform source and sink terms in the convective domain consistent with the lateral entrainment and detrainment of mass implied by $w_{swtg}$, as described in *Herman and Raymond* [2014]. Reference mixing ratio and moist entropy profiles $r_R(z)$ and $s_R(z)$ serve to specify the humidity and moist entropy of the air being entrained into the convective domain from the environment.

*Wang and Sobel* [2012] treat the effect of environmental humidity on their WTG model by relaxing the convective domain toward a dry reference profile in order to mimic the effect of dry advection on the convection. The philosophy taken in the present work is that the time constant for advective relaxation is much greater than the time constant of a convective cell. In this case the effect of moisture advection is represented indirectly by the actual reference profile and including an additional drying (or moistening) via this type of relaxation would be redundant.

A two-dimensional version of the cloud model was used to make possible a large number ($\approx 100$) of model runs with different environmental conditions. A domain of 192 km in the horizontal by 20 km in the vertical was used with a grid box size of 1000 m $\times$ 250 m. A sponge layer was used in the uppermost 5 km to damp gravity wave reflections and periodic lateral boundary conditions were imposed.

Zero ambient wind in the $x$ direction was specified and the horizontal mean of the convective domain wind was relaxed toward this initial profile to suppress the effects of counter-gradient momentum transfer that tends to occur in two-dimensional models of convection.

**Table 1.** Important Cloud Model Parameters

| Parameter | Value | Comment |
|---|---|---|
| eddy | 1.0 | coefficient for eddy mixing |
| filter | 0.003 | strength of horizontal 2*dx filter |
| lambda | 0.001 | strength of vertical hypersmoothing |
| crain | $0.01\,\text{s}^{-1}$ | rain production constant |
| csnow | $0.01\,\text{s}^{-1}$ | ice production constant |
| cevap | $1.0\,\text{s}^{-1}$ | precipitation evaporation constant |
| wtermw | $5.0\,\text{ms}^{-1}$ | rain terminal velocity |
| wtermi | $5.0\,\text{ms}^{-1}$ | ice terminal velocity |
| radcool | $1.5\,\text{Kd}^{-1}$ | radiative cooling rate |
| cdrag | 0.001 | surface drag coefficient |
| ueffmin | $3.0\,\text{ms}^{-1}$ | surface gustiness parameter |
| hscale ($L$) | $1.5{\times}10^5\,\text{m}$ | SWTG horizontal scale |

Table 1 lists important cloud resolving model constants. See *Herman and Raymond* [2014] for more information. Fixed radiation was used, with a constant radiative cooling rate of $1.5\,\text{Kd}^{-1}$ up to 12 km and a linear decay to zero at an elevation of 15 km.

The cloud physics parameterization is primitive by design, allowing simple sensitivity tests to be made. Liquid and solid precipitation are treated equally with $5\,\text{ms}^{-1}$ terminal velocities for both, so the cloud physics of snow that is needed to produce stratiform rain areas is not currently included. A constant drag coefficient that is the same for both momentum and thermodynamic transfers is also used in conjunction with constant gustiness parameter.

### 2.2. Model Runs

Model runs were made in two dimensions on a 192 km×20 km domain with grid cells of dimensions 1 km×250 m. A long ($10^7\,\text{s} \approx 116\text{d}$) radiative-convective equilibrium (RCE) integration of the model with an SST of 300 K and wind normal to the model plane of $v_y=5\,\text{ms}^{-1}$ was done and initial RCE profiles were obtained by averaging this output over the last $8{\times}10^6\,\text{s} \approx 93\text{d}$. This integration was itself initialized from a previous RCE run made under the same conditions, so the integration started out very close to RCE. These measures were needed to produce a very accurate initial RCE profile, as small errors can produce deleterious effects on subsequent SWTG runs.

Reference profiles for the SWTG calculations were obtained by perturbing the initial RCE temperature, humidity, and $v_y$ wind profiles as well as imposing a range of SSTs. (The $x$ component of the reference wind is set to zero.) Values of $v_y=0, 3, 5, 7, 10, 15, 20\,\text{ms}^{-1}$ (independent of height) and SST $=299, 300, 301$ K were used. Note that since the model is two-dimensional in the $x$–$z$ plane and the Coriolis force is set to zero, The $v_y$ wind component has no effect on the model results except in the calculation of the reference surface entropy fluxes.

The potential temperature and relative humidity reference profiles were varied by imposing perturbations composed from basis functions consisting of the positive halves of the $n = 0, 2, 4$ wave functions of the quantum mechanical harmonic oscillator [*Schiff*, 1955]. These functions are mutually orthogonal and are shown in Figure 1.

Potential temperature and relative humidity perturbations were treated slightly differently. The potential temperature reference profiles $\theta_R(z)$ were obtained from

$$\theta_R(z)=\theta_0(z)+T_0M_0+T_2M_2+T_4M_4 \tag{8}$$

whereas the relative humidity reference profiles $H_R(z)$ were created using

$$H_R(z)=H_0(z)[1+R_0M_0+R_2M_2+R_4M_4]. \tag{9}$$

The quantities $\theta_0(z)$ and $H_0(z)$ are the initial RCE profiles of potential temperature and relative humidity, the $M_i(z)$ are the basis functions shown in Figure 1, and the $T_i$ and $R_i$ are coefficients determining the contributions of each mode to the respective reference profiles. The relative humidity perturbations are multiplicative to reduce the possibility of generating relative humidities less than 0 or greater than 1.

The three basis functions used can represent only the coarse vertical structure of the potential temperature and relative humidity perturbations. However, experiments with fine-scale perturbations of these quantities suggest that they tend to be less important than the gross features of the profiles, at least if the perturbation amplitudes are relatively small. In the tropics, one expects relatively weak perturbations to the potential temperature profile to exist due to the tendency of buoyancy anomalies to be smoothed out by gravity wave action. The same may be true of
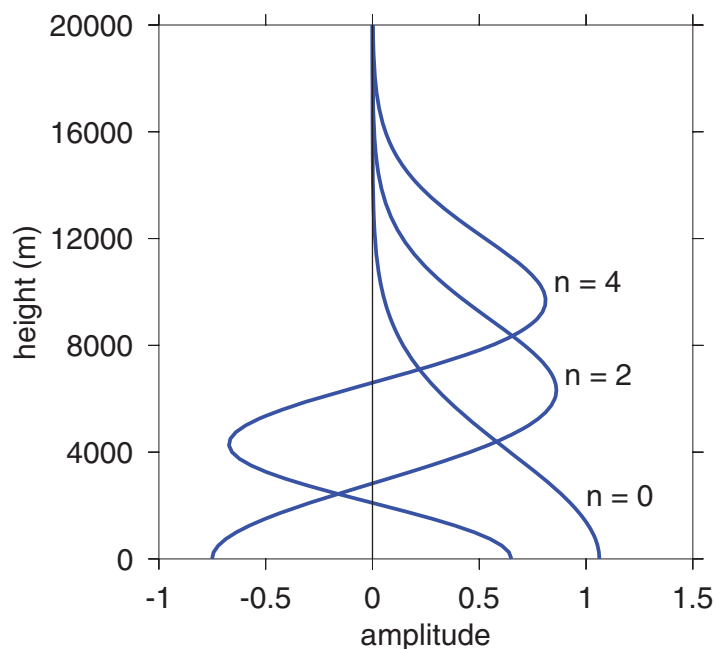
**Figure 1.** Orthogonal basis functions for potential temperature and relative humidity reference profile perturbations.

moisture profiles in the vicinity of deep convection due to a process of moisture quasi-equilibrium [*Raymond et al.*, 2014], though not in convection-free regions.

The strategy used to minimize the parameter phase space needing coverage is to assume that the rainfall rate is a linear function of the reference surface wind speed $v_y$, the SST, and the thermodynamic profile coefficients $T_i$ and $R_i$. Note that the surface evaporation rate and moist entropy flux are implied by these variables.

The linearity assumption is likely to be true as long as the deviations from RCE are in some sense "small," with the exception of cases in which the rainfall rate goes to zero. Other than that special case, what constitutes "small enough" is not known *a priori* and must be tested *a posteriori*. The linearity assumption allows parameters to be perturbed one at a time. However, since the assumed surface wind speeds cover a large range, we varied all of the other parameters for each value of wind speed. Figure 2 shows the values assumed for $T_i$ and $R_i$ as a function of wind speed for the SST equal to 300 K. For 299 K and 301 K we ran only the cases with $T_i, R_i = 0$.

SWTG calculations were run for $5 \times 10^6$ s, averaging over the last $3 \times 10^6$ s for all members of the above-defined parameter space. This long ($\approx 35$d) averaging period results in accurate estimates of the average rainfall rate produced for each simulation.

## 3. Results

The main purpose of this paper is to determine how environmental factors control space and time averaged precipitation. The word *control* implies determination of causality. The reference profiles of temperature, humidity, and wind, SST, and in the present case radiation, are externally imposed, and therefore ought to control the behavior of the model. However, there are limits to this control.

The small space and time scale details of convection, and hence rainfall, are turbulent and hence unpredictable. However, in most cases the long-term time and space averages of convective behavior are uniquely determined by the reference conditions, which can therefore be thought of as controlling average convective behavior.

An exception occurs where multiple equilibria exist in simulated convection, generally with two different equilibrium states, a moist, rainy equilibrium and a state of low humidity and no rain [*Sobel et al.*, 2007; *Raymond et al.*, 2009; *Sessions et al.*, 2010]. Using the traditional WTG model, *Sessions et al.* [2015] showed that fixed radiation produces multiple equilibria over a smaller range of input parameters than interactive radiation. In addition, our experience is that SWTG is even less susceptible to multiple equilibria than traditional WTG for fixed radiation, so multiple equilibria are likely to be of little or no importance in the present results.

Based on previous work on tropical cyclone formation, e.g., *Gjorgjievska and Raymond* [2014], the dimensionality of the causal parameter space is vastly reduced by assuming that the saturation fraction and instability index (both defined in section 2) characterize the temperature and humidity profiles.
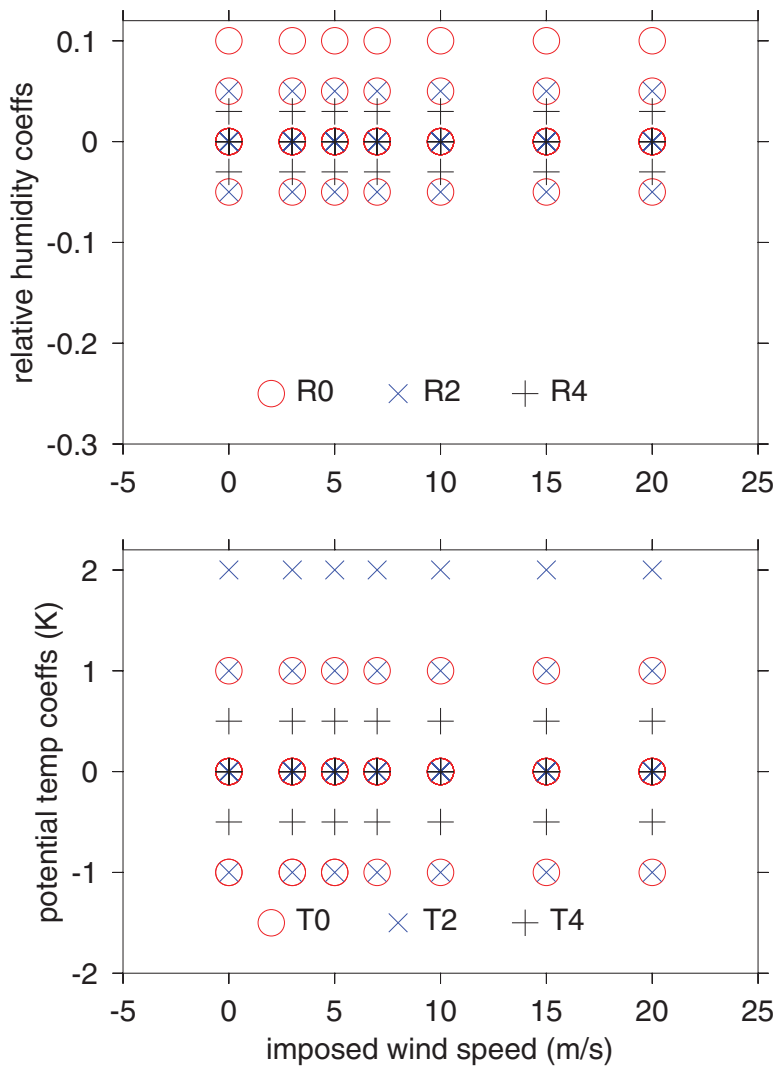
**Figure 2.** Potential temperature and relative humidity coefficients used in calculations with SST =300K.

Other likely causal parameters are the surface evaporation rate and moist entropy flux as well as the SST. Variations of $\pm 1$ K in the SST account for a very small fraction of the variance in the rainfall rate independent of their contribution to variations in surface thermodynamic fluxes in the present set of simulations. Furthermore, the surface moist entropy flux and the surface evaporation rate are correlated at the 99% level, and are therefore not independent. These two factors allow us to further collapse the parameter space by replacing the SST and the surface wind speed by a single parameter, which we choose to be the surface moist entropy flux. Thus, we hypothesize that the reference values of surface moist entropy flux (eflux), instability index (II), and saturation fraction (SF) are sufficient to characterize the time and space averaged rainfall rate in the model.

Figure 3 shows a scatter plot of the predicted versus the actual rainfall rate in the ensemble of runs with rainfall exceeding 1 mm d$^{-1}$. The predicted rainfall is based on a linear regression with the above reference variables. Nonprecipitating cases are excluded from the regression but included in the plot. The prediction equation for rainfall based on this regression is
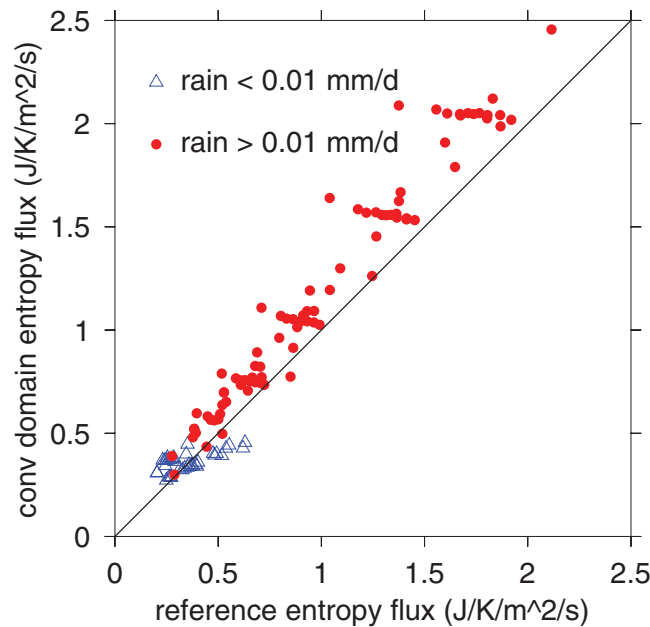
$$R_P = -251 + 45.8; \text{eflux} - 1.02; \text{II} + 362; \text{SF} \tag{10}$$

where the predicted rainfall $R_P$ is in millimeters per day and the other quantities are in standard SI units.
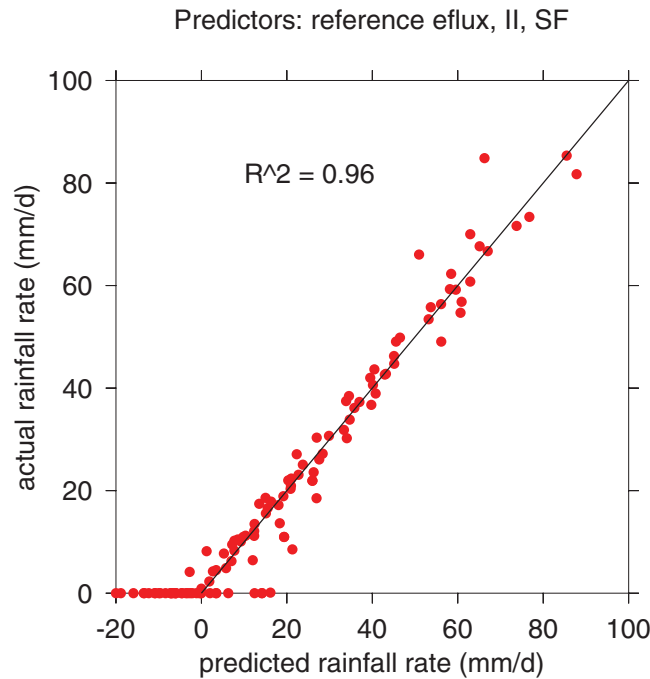
**Figure 3.** Predicted versus actual model rainfall based on a linear regression for the predicted rain with the reference values of surface moist entropy flux, instability index, and saturation fraction as the predictor variables. 96% of the variance is accounted for.

The surface entropy flux by itself explains 69% of the variance, while adding in the instability index results in 84% explained. The saturation fraction raises the total to 96%. Thus, these three reference variables account for a rather large fraction of average rain production in the model.
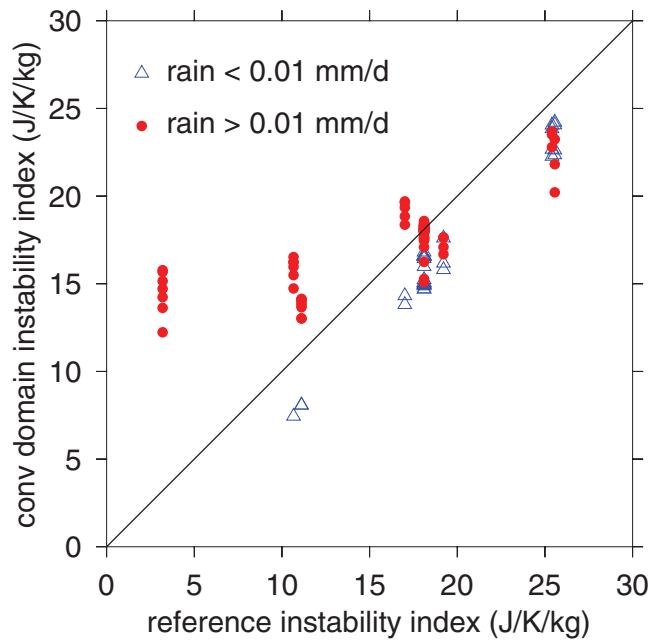
Averages of these three parameters over the convective domain are not necessarily equal to the corresponding reference profile values. We now explore how reference and convective domain values compare with each other.

Figure 4 shows a scatter plot of reference versus convective domain surface moist entropy flux over the ensemble of model runs. The convective domain values are generally larger than the reference profile values by approximately 15%, especially when precipitation is occurring. This is presumably due to the fact that gustiness produced by the convection can increase the fluxes over those present in the undisturbed convective environment. *Jabouille et al*. [1996] found that convective gustiness produced the strongest anomalies in surface latent heat fluxes in light wind situations, with values up to $50 \text{ms}^{-1}$ ($\approx 0.17 \text{JK}^{-1}\text{m}^{-2}\text{s}^{-1}$ in terms of the moist entropy flux). Given other possible factors in our analysis, this is a relatively minor effect. The nonprecipitating cases tended to have small values of the surface entropy flux and large values of the instability index.

Figure 5 shows the convective domain versus the reference profile instability indices. There is some random scatter between the two, though the main effect is a compression in the range of convective domain values relative to reference values.

The situation for saturation fraction is somewhat more complicated. Figure 6 shows a scatter plot of reference versus convective domain saturation fraction. Though there is weak correlation between the two quantities for precipitating cases, in the absence of precipitation there is basically no correlation at all. Furthermore, the spread in convective domain values is large compared to the spread in reference values. This suggests that convective and radiative processes have large



**Figure 4.** Relationship between reference and convective domain values of the surface moist entropy flux. Precipitating and nonprecipitating cases are distinguished by red dots and blue triangles respectively.

**Figure 5.** Relationship between reference profile and convective domain values of instability index. Precipitating and nonprecipitating cases are distinguished by red dots and blue triangles respectively.
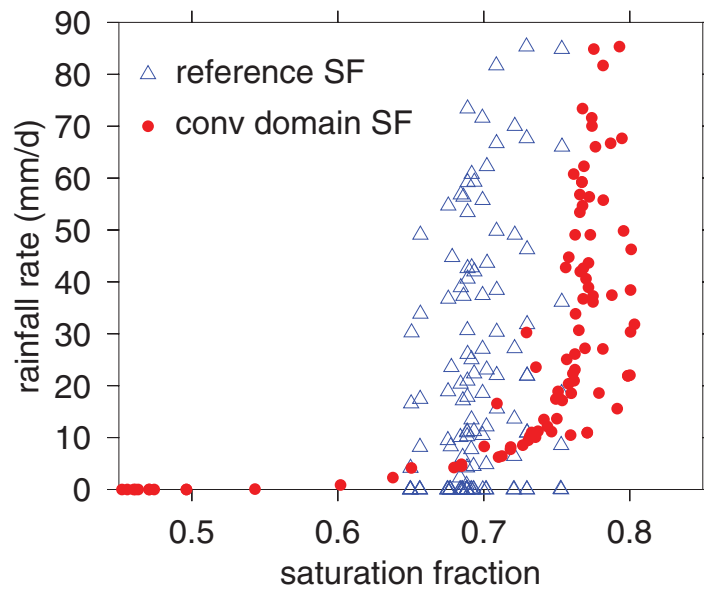
effects on the convective domain saturation fraction irrespective of the reference values.

Figure 7 shows plots of rainfall rate versus reference and convective domain saturation fraction. The latter exhibits a "hockey stick" curve with rapidly increasing rainfall above a saturation fraction of about 0.7, as found in observations by *Bretherton et al.* [2004] and many others. In contrast, the reference profile saturation fraction values are limited to the range 0.65–0.75 with only a slight correlation with rainfall rate.

Figure 8 shows that convective domain saturation fraction and instability index are strongly anti-correlated for large values of the rainfall rate. This is in agreement with observations of convection in potential precursor disturbances for tropical cyclones [*Gjorgjievska and Raymond*, 2014]. We ascribe these results to a "moisture quasi-equilibrium" process as outlined by *Singh and O'Gor-*

*man* [2013]. If the environment is dry, then convection requires larger values of parcel buoyancy to withstand environmental entrainment and evaporation of condensate than when the environment is more moist. Larger parcel buoyancy corresponds to larger instability index. If the environment is too dry to sustain convection for a given value of instability index, then clouds detrain their moisture and decay, thus moistening the environment. On the other hand, if the environment is too moist, then convection is more vigorous and the resulting precipi-
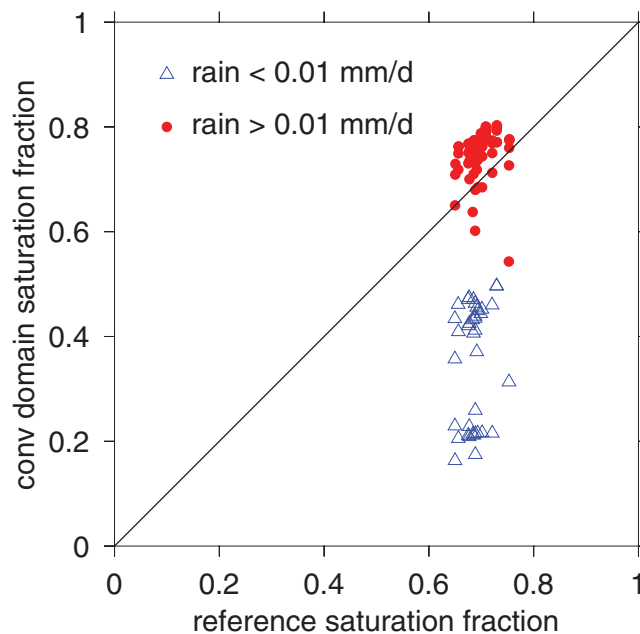


**Figure 6.** Relationship between reference profile and convective domain values of saturation fraction. Precipitating and nonprecipitating cases are distinguished by red dots and blue triangles respectively.

tation dries out the atmospheric column. The net effect is the relaxation of the humidity profile to some optimum value between these two extremes. The optimum humidity becomes drier as the instability becomes greater.

Modeling of convection by *Singh and O'Gorman* [2013] shows that convection adjusts the model environment to produce very close to zero buoyancy for subsequent convection. In a model this could result from the convection altering either the environmental humidity or the moist convective instability. However, in the real world the environment is continually adjusting to produce a balanced temperature profile and associated value of the instability index. Thus, on time scales longer than the dynamical adjustment time scale, the convection controls only the humidity since larger-scale dynamics regulates the convective instability. Greater instability therefore

**Figure 7.** Relationship between reference (blue triangles) and convective domain values (red dots) of saturation fraction and rainfall.

yields a drier atmosphere whereas less instability results in higher humidities. This explains the inverse relationship between instability index and saturation fraction seen for large rainfall rates in Figure 8 and in observational results.

*Raymond* [2000] developed a simple model of what is now called moisture quasi-equilibrium. The moisture relaxation time in the case of weak convection characteristic of the radiative-convective equilibrium state is a few weeks. However, this relaxation time scales as the inverse square of the convective strength, as measured by the average precipitation rate. For very strong convection it decreases to less than 1 day. This explains why moisture quasi-equilibrium only holds for large rainfall rates in Figure 8.

If the convection is weak, then the above analysis suggests that the saturation fraction is an independent predictor variable for precipitation. As the convection becomes stronger, then the saturation fraction becomes more closely tied with the instability index. In this case, the saturation fraction becomes redundant as a predictor.

We now test this hypothesis with respect to our ensemble of model runs. Figure 9 shows that 91% of the variance in the rainfall is predicted by the surface moist entropy flux and the instability index. This almost as high as the regression results for reference values of surface entropy flux, instability index, and saturation fraction shown in Figure 3. However, there is a tendency for a few nonprecipitating cases to exhibit large predicted values of precipitation. (As with reference value test, nonprecipitating cases are omitted from the regression, though they are still displayed.) The predicted rain in terms of the surface moist entropy flux and instability index is

$$R_P = 46 + 38.8; \text{eflux-}3.49; \text{II}. \qquad (11)$$

A regression with just surface moist entropy flux results in 79% of the variance explained, which means that instability index adds significant information. On the other hand, adding the model domain saturation fraction to the list of predictor variables results in little new information (92% of variance
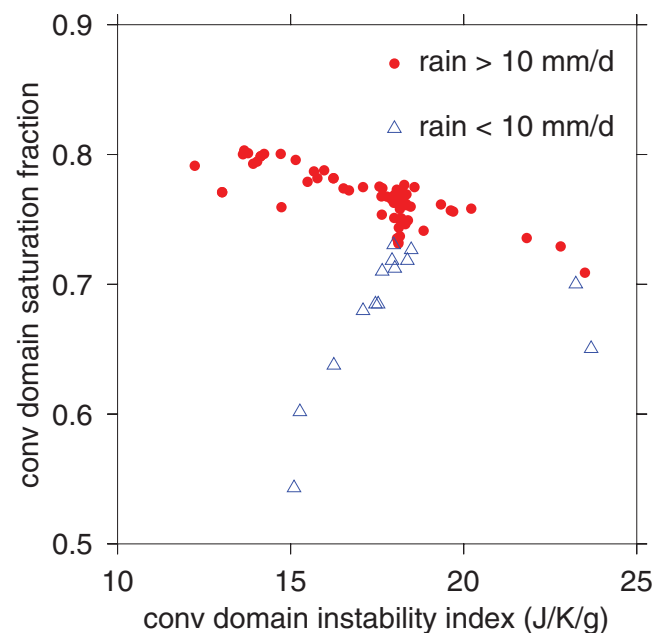


**Figure 8.** Scatter plot of convective domain saturation fraction and instability index for the simulations discussed in this paper. The cases are separated into two categories, those with rainfall rates greater than 10 mm d$^{-1}$ and those with less than this value.

### Predictors: convective domain eflux, II
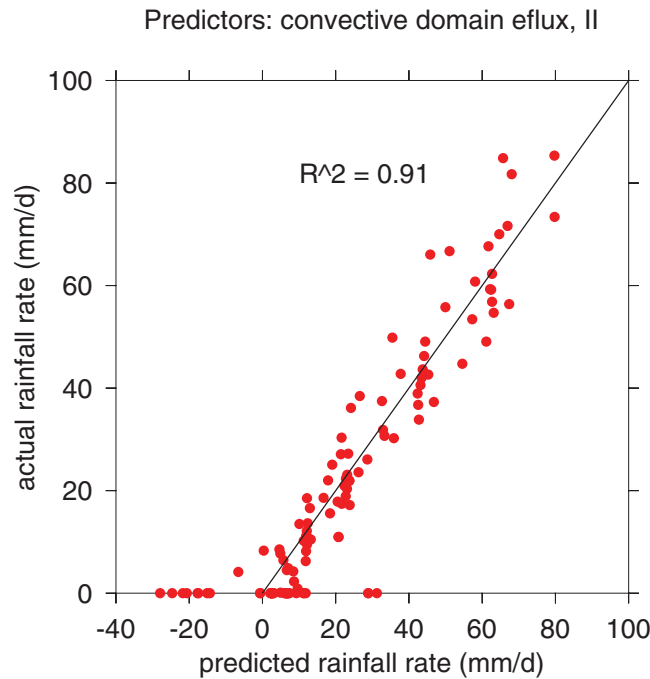


**Figure 9.** As in Figure 3 with convective domain surface moist entropy flux and instability index taken as predictor variables. 91% of the variance in rainfall is explained by the regression.

explained) in comparison to just the surface flux and instability index (see Figure 10). The main effect of the saturation fraction is in tidying up the results for low rainfall rates. The cases with actual zero rain now take on negative predicted rainfall. These results are in accord with the hypothesis that saturation fraction is only an independent predictor at low rainfall rates where the moisture relaxation time constant is large. The rain predicted by the regression is given by

$$R_P = -28 + 36.4; \text{eflux-}2.67; \text{II} + 83.3; \text{SF}. \tag{12}$$

## 4. Comparison With Observations

Comparing SWTG results with observations is tricky, as one must decide whether reference values of entropy flux, instability index, and saturation fraction or the corresponding convective domain values should be used in the comparison. In principle, the former should be used if the observations are of the clear regions surrounding the convection, while the latter would be more appropriate if detailed observations in the immediate vicinity of the convection were available.

### Predictors: convective domain eflux, II, SF
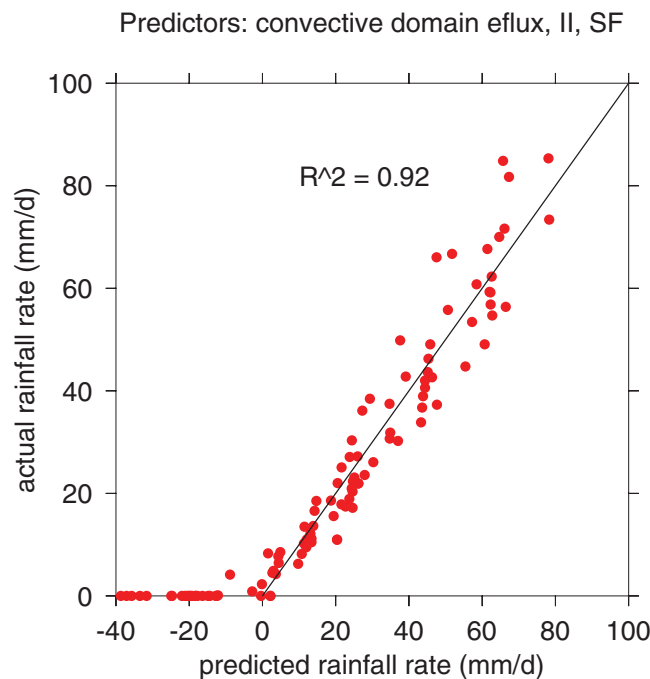


**Figure 10.** As in Figure 9 except with the convective domain saturation fraction added as an independent variable. 92% of the variance is explained.

If one is concerned about understanding the causes of convection, then the focus should be on reference values, since these are unambiguously causal in the SWTG model; the convective domain values are significantly affected by the convection itself, especially the saturation fraction. The control of convection over the instability index and the surface entropy flux is weaker but still significant.

Two comparisons are made below, one with the analysis of mesoscale dropsonde observations of tropical convective disturbances, the other with the results of global analyses.

### 4.1. TCS08 and PREDICT

In this section, we compare the predictions derived from the model to observations of convection in 37 cases of tropical disturbances in the western Pacific (Tropical Cyclone Structure experiment (TCS08)) [*Elsberry and Harr*, 2008] and the western Atlantic and
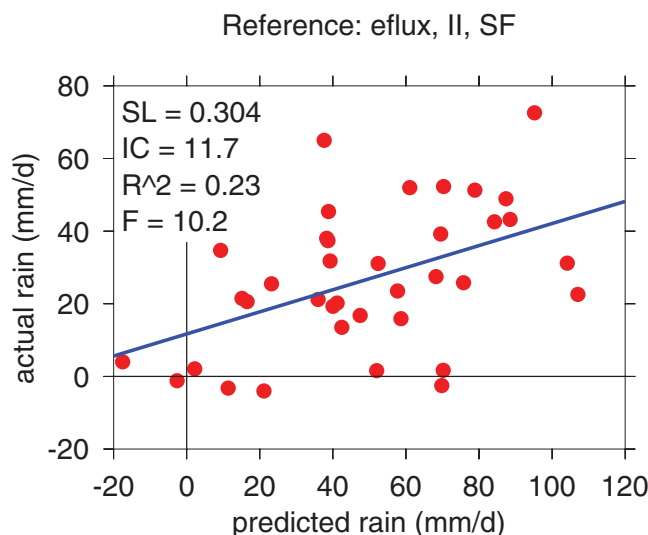
**Figure 11.** Actual rainfall from TCS08 and PREDICT plotted against the observed rainfall using the model based on reference values of parameters. SL and IC represent the slope and y intercept of the blue regression line while $R^2$ and F represent the fraction of variance accounted for by the regression and the F statistic.

Caribbean (Pre-Depression Investigation of Cloud-Systems in the Tropics (PREDICT)) [*Montgomery et al.*, 2012]. These observations are taken from dropsonde grids over domains a few degrees in diameter with resolution of order one degree and are described by *Gjorgjievska and Raymond* [2014]. In these cases rainfall was not actually measured. We therefore use observed moisture convergence plus surface evaporation rate, averaged over a box typically a few degrees in diameter, as a proxy for rainfall, which for convenience we simply call "rainfall." This proxy omits the effect of the time tendency of precipitable water in the moisture budget, thus introducing noise. Additional noise comes from the fact that the instantaneous rainfall rate itself is noisy relative to the long-term average rainfall extracted from the model. For this reason, the very high values of explained variance in the model results cannot be expected in the application of the model predictions of rainfall to the observational results.

Examination of fields of instability index and saturation fraction in the observational results shows extreme variability in these quantities over scales of 10–100 km. In many cases the averages of these quantities over the observed domain are dominated by the environment surrounding the convection of interest. This supports the use of the precipitation model based on reference rather than convective domain values, though it is admittedly difficult to make a clean separation between near and far convective environment in the observations.

In order to evaluate the results of our precipitation predictions against these observations, we compute a further regression between observed rainfall and rainfall predicted from the observationally derived parameters using the reference profile model given by (10). Figure 11 shows actual rainfall as a function of model-predicted rainfall in this case. 23% of the variance in observed rainfall is explained by this model. The value of the F statistic is 10.2, which means that the correlation is significant at greater than the 99% level.

The rainfall prediction model therefore shows skill in predicting rainfall for the TCS08-PREDICT cases. However, the prediction has offset and scaling errors. The offset error can be easily ascribed to differences in the thermodynamics of the model compared to the real world. However the scaling error results in an overprediction of precipitation by a factor of 3 once the offset error is accounted for. The error may be a result of simplifications in the model such as two-dimensionality and fixed radiation. This bears further investigation.

The rainfall prediction using convective domain values of entropy flux, instability index, and saturation fraction was also tested against this data set (not shown). The results are similar to the reference profile case, though the skill is less, with 17% of the rainfall variance accounted for. The offset and scaling errors are greater, with a scaling overprediction by a factor of 4. These results support the use of the rainfall prediction model based on reference parameters, though extra skill exhibited in that case is small.
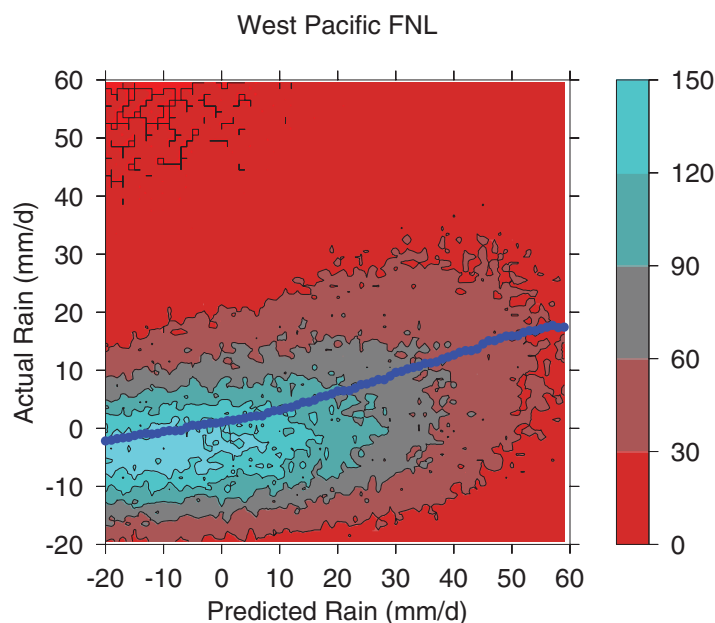
### 4.2. Global Analyses

We now test our precipitation prediction algorithm against the National Centers for Environmental Prediction's Final Operational Global Analysis data set (FNL; http://rda.ucar.edu/datasets/ds083.2/). Since the FNL does not provide precipitation, we use the same precipitation proxy as in the TCS08-PREDICT data set
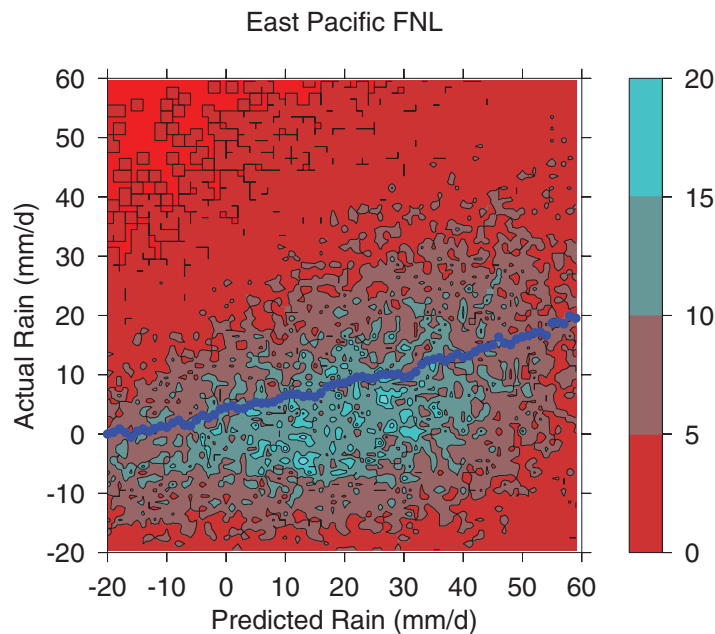
**Figure 12.** Number density distribution of FNL values of the "actual" rainfall (moisture convergence plus surface evaporation) versus the predicted rainfall from (10) for June–August 2015 in the east Pacific ([110–90 W], [8–13 N]). The blue line indicates the weighted average of the actual rainfall as a function of the predicted rainfall.

("actual rainfall"), namely the vertically integrated moisture convergence plus the surface evaporation rate. The reference parameter precipitation prediction equation (10) is also used here.

Figure 12 shows the number density distribution of values of the actual versus predicted rainfall derived from the FNL for the summertime tropical east Pacific at and north of the intertropical convergence zone. The blue line shows the distribution-weighted average of the actual rainfall as a function of predicted rainfall. A similar plot for the northern summer northwest Pacific is shown in Figure 13.

The two cases are very similar, though the smaller data sample in the east Pacific case makes the number distribution noisier.

In both cases the average actual rain is larger than the peak in the distribution because the distributions are skewed toward larger values of actual rainfall. The average lines in both cases are nearly linear, but with offset and scaling errors. The offsets are small and the scaling errors imply predicted values of order 3 times actual values in both cases as in the TCS08-PREDICT results. Similar results are obtained from the ERA-Interim reanalysis [*Dee et al.*, 2011] (not shown).

## 5. Discussion and Conclusions

The spectral version of our cloud resolving model with a weak temperature gradient parameterization of the large-scale flow is used to evaluate the environmental conditions that control time and space-averaged convective precipitation rates over tropical oceans. Over 100 two-dimensional simulations with fixed radiative cooling are used to span the range of variations in environmental conditions that is likely to be found over warm tropical oceans. The first step is to calculate closed domain radiative-convective equilibrium profiles of temperature and humidity at fixed values of SST and imposed



**Figure 13.** As in Figure 12 except for the northwest Pacific ([130–180 E], [0–23 N]).

surface wind speed. The second step is to use these thermodynamic profiles and this SST as reference conditions in weak temperature gradient calculations over the range of imposed imposed winds of 0–20 ms$^{-1}$. For each of these wind values, further calculations are then made in which the thermodynamic profiles and SST are varied systematically.

Even with this large number of simulations, filling the parameter space is only possible if certain assumptions are made. The first is that temperature and humidity perturbations about the previously calculated radiative-convective equilibrium state are assumed to have a coarse vertical structure, i.e., with only 3 degrees of freedom each. *A posteriori* tests suggest that perturbations with fine vertical structure are not important as long as their amplitude is not too large. An additional critical assumption is that the imposed deviations are small enough that resulting changes in the rainfall are linear functions of the deviations. This allows us to explore the effect of changing parameters one at a time, which results in a further large reduction in the size of the parameter space. Tests indicate that this assumption is largely justified, given the size of perturbations employed.

Observational results suggest that an additional reduction in the parameter space is possible. The saturation fraction, which is essentially a column-averaged relative humidity, has a close relationship to precipitation over warm tropical oceans. The instability index, which measures lower tropospheric moist convective instability, is closely related to first baroclinic mode temperature perturbations. Variations in SST and imposed surface wind speed collapse into variations in the surface evaporation rate and surface moist entropy flux. Furthermore, over tropical oceans, these two surface fluxes covary to a high degree of accuracy. This leaves us with three important parameters that potentially control precipitation, one of the two surface fluxes, which we choose to be the moist entropy flux, the instability index, and the saturation fraction.

We next address causality. Within the confines of the model, the values of entropy flux, instability index, and saturation fraction derived from reference thermodynamic and wind profiles are unambiguously causal; variations in these externally imposed parameters explain 96% of the variance in the precipitation over the range of model simulations used in the analysis. Convective domain values of the above parameters are affected by the convection itself and to varying degrees covary with the precipitation and are therefore not causal.

Comparison of our results with observations from two field programs and with the FNL analysis and ERA-Interim reanalysis suggests that a linear precipitation model based on the reference values of surface moist entropy flux, instability index, and saturation fraction exhibits significant skill in predicting actual mean rainfall. However, the prediction has offset and scaling errors, the most significant of which being the over-prediction of average rain by roughly a factor of 3. This factor is consistent across the different observational cases. Simplifying assumptions made in the model simulations, e.g., two-dimensionality and fixed radiation, could be responsible for this discrepancy. Further work is needed here.

Differences between reference and convective domain values of our parameters are enlightening. In our modeling results, the convective domain values of the surface moist entropy flux tend to be modestly larger than reference values.

Somewhat more variability exists between reference and convective domain values of the instability index; convective domain values tend to be larger than reference values, especially for small reference values. The tendency for gravity wave action to homogenize temperature profiles in the tropics also results in a tendency to homogenize the instability index, since it depends solely on the temperature profile. Thus, reference and convective domain values of this parameter should not differ too much from each other in most cases.

The situation with saturation fraction is altogether different. No large-scale restorative processes exist for water vapor and there is very little correlation between the reference and convective domain values of the saturation fraction. There is, however, a strong negative correlation between saturation fraction and instability index that reflects a convective process referred to as moisture quasi-equilibrium; moister atmospheres in convective regions are more stable and vice versa. Therefore, convective domain saturation fraction is not a predictive variable for precipitation in regions of strong convection; it simply covaries with the precipitation itself and in some ways can be considered a surrogate for precipitation.

Moisture quasi-equilibrium breaks down when convection is weak or nonexistent. In this case saturation fraction becomes an important predictive parameter; if the environment is too dry, precipitation cannot occur no matter how favorable the other predictive parameters are.

Since saturation fraction covaries with instability index in strong convection and becomes an independent predictive parameter in weak convection, there is no harm in including it as a predictive parameter for precipitation. As a comparison of Figures 9 and 10 shows, its inclusion does basically nothing in heavy rain and plays the constructive role of eliminating predictions of heavy rain when the actual rain is light or nonexistent.

We conclude that the average rainfall in a weak temperature gradient convective model can be predicted by a combination of externally imposed values of only three parameters, the surface moist entropy flux, the instability index, and the saturation fraction. Furthermore, the equation thus derived exhibits skill in predicting average convective rainfall over tropical oceans, though scaling and offset errors must be accounted for to make these predictions quantitative. Further work is needed to track down the source of these errors and to extend comparisons to a broader range of observational cases.

## References

Back, L. E., and C. S. Bretherton (2005), The relationship between wind speed and precipitation in the Pacific ITCZ, *J. Clim.*, *18*, 4317–4328.

Bretherton, C. S., and P. K. Smolarkiewicz (1989), Gravity waves, compensating subsidence and detrainment around cumulus clouds, *J. Atmos. Sci.*, *46*, 740–759.

Bretherton, C. S., M. E. Peters, and L. E. Back (2004), Relationships between water vapor path and precipitation over the tropical oceans, *J. Clim.*, *17*, 1517–1528.

Dee, D. P., et al. (2011), The ERA-Interim reanalysis: Configuration and performance of the data assimilation system, *Q. J. R. Meteorol. Soc.*, *137*, 553–597, doi:10.1002/qj.828.

Dorrestijn, J., D. T. Crommelin, A. P. Siebesma, H. J. J. Jonker, C. Jakob (2015), Stochastic parameterization of convective area fractions with a multicloud model inferred from observational data, *J. Atmos. Sci.*, *72*, 854–869.

Elsberry, R. L., and P. A. Harr (2008), Tropical cyclone structure (TCS08) field experiment science basis, observational platforms, and strategy, *Asia Pac. J. Atmos. Sci.*, *44*, 209–231.

Emanuel, K. A. (1986), An air-sea interaction theory for tropical cyclones. Part I: Steady state maintenance, *J. Atmos. Sci.*, *43*, 585–604.

Emanuel, K. A. (1987), An air-sea interaction model of intraseasonal oscillations in the tropics, *J. Atmos. Sci.*, *44*, 2324–2340.

Gjorgjievska, S., and D. J. Raymond (2014), Interaction between dynamics and thermodynamics during tropical cyclogenesis, *Atmos. Chem. Phys.*, *14*, 3065–3082.

Groenemeijer, P., and G. C. Craig (2012), Ensemble forecasting with a stochastic convective parameterization based on equilibrium statistics, *Atmos. Chem. Phys.*, *12*, 4555–4565, doi:10.5194/acp-12-4555-2012.

Herman, M. J., and D. J. Raymond (2014), WTG cloud modeling with spectral decomposition of heating, *J. Adv. Model. Earth Syst.*, *6*, 1121–1140, doi:10.1002/2014MS000359.

Jabouille, P., J. L. Redelsperger, and J. P. Lafore (1996), Modification of surface fluxes by atmospheric convection in the TOGA COARE region, *Mon. Weather Rev.*, *124*, 816–837.

Khairoutdinov, M., D. Randall, and C. Demott (2005), Simulations of the atmospheric general circulation using a cloud-resolving model as a superparameterization of physical processes, *J. Atmos. Sci.*, *62*, 2136–2154.

Khairoutdinov, M., C. Demott, and D. Randall (2008), Evaluation of the simulated interannual and subseasonal variability in an AMIP-style simulation using the CSU multiscale modeling framework, *J. Clim.*, *21*, 413–431.

Khouider, B., J. Biello, and A. J. Majda (2010), A stochastic multicloud model for tropical convection, *Commun. Math. Sci.*, *8*, 187–216.

Komaromi, W. A. (2013), An investigation of composite dropsonde profiles for developing and nondeveloping tropical waves during the 2010 PREDICT field campaign, *J. Atmos. Sci.*, *70*, 542–558.

Lin, J. W.-B., and J. D. Neelin (2003), Toward stochastic deep convective parameterization in general circulation models, *Geophys. Res. Lett.*, *30*(4), 1162, doi:10.1029/2002GL016203.

Lindzen, R. S. (1974), Wave-CISK in the tropics, *J. Atmos. Sci.*, *31*, 156–179.

Maloney, E. D., and A. H. Sobel (2004), Surface fluxes and ocean coupling in the tropical intraseasonal oscillation, *J. Clim.*, *17*, 4368–4386.

Montgomery, M. T., et al. (2012), The pre-depression investigation of cloud systems in the tropics (PREDICT) experiment, *Bull. Am. Meteorol. Soc.*, *93*, 153–172.

Ooyama, K. (1969), Numerical simulation of the life cycle of tropical cyclones, *J. Atmos. Sci.*, *26*, 3–40.

Ooyama, K. (1982), Conceptual evolution of the theory and modeling of the tropical cyclone, *J. Meteorol. Soc. Jpn.*, *60*, 369–379.

Palmer, T. N. (2001), A nonlinear dynamical perspective on model error: A proposal for non-local stochastic-dynamic parameterization in weather and climate model predictions, *Q. J. R. Meteorol. Soc.*, *127*, 279–304.

Peters, K., C. Jakob, L. Davies, B. Khouider, and A. J. Majda (2013), Stochastic behavior of tropical convection in observations and a multi-cloud model, *J. Atmos. Sci.*, *70*, 3556–3575.

Plant, R. S., and G. C. Craig (2008), A stochastic parameterization for deep convection based on equilibrium statistics, *J. Atmos. Sci.*, *65*, 87–105.

Raymond, D. J. (1995), Regulation of moist convection over the west Pacific warm pool, *J. Atmos. Sci.*, *52*, 3945–3959.

Raymond, D. J. (2000), Thermodynamic control of tropical rainfall, *Q. J. R. Meteorol. Soc.*, *126*, 889–898.

Raymond, D. J., and K. A. Emanuel (1993), The Kuo cumulus parameterization, in *The Representation of Cumulus Convection in Numerical Models*, edited by K. A. Emanuel and D. J. Raymond, pp. 145–147, Am. Meteorol. Soc., Boston, Mass.

Raymond, D. J. and S. L. Sessions (2007), Evolution of convection during tropical cyclogenesis, *Geophys. Res. Lett.*, *34*, L06811, doi:10.1029/2006GL028607.

Raymond, D. J., and X. Zeng (2005), Modelling tropical atmospheric convection in the context of the weak temperature gradient approximation, *Q. J. R. Meteorol. Soc.*, *131*, 1301–1320.

Raymond, D. J., G. B. Raga, C. S. Bretherton, J. Molinari, C. López-Carrillo, and Ž. Fuchs (2003), Convective forcing in the intertropical convergence zone of the eastern Pacific, *J. Atmos. Sci.*, *60*, 2064–2082.

Raymond, D. J., C. S. Bretherton, and J. Molinari (2006), Dynamics of the intertropical convergence zone of the east Pacific, *J. Atmos. Sci.*, *63*, 582–597.

Raymond, D. J., S. Sessions, A. Sobel, and Ž. Fuchs (2009), The mechanics of gross moist stability, *J. Adv. Model. Earth Syst.*, *1*, 9, doi:10.3894/JAMES.2009.1.9.

Raymond, D. J., S. L. Sessions, and C. López Carrillo (2011), Thermodynamics of tropical cyclogenesis in the northwest Pacific, *J. Geophys. Res.*, *116*, D18101, doi:10.1029/2011JD015624.

Raymond, D. J., S. Gjorgjievska, S. Sessions, and Ž. Fuchs (2014), Tropical cyclogenesis and mid-level vorticity, *Aust. Meteorol. Oceanogr. J.*, *64*, 11–25.

Raymond, D. J., Ž. Fuchs, S. Gjorgjievska, and S. L. Sessions (2015), Balanced dynamics and convection in the tropical troposphere, *J. Adv. Model. Earth Syst.*, *7*, 1093–1116, doi:10.1002/2015MS000467.

Schiff, L. I. (1955), *Quantum Mechanics*, 2nd ed., 417 pp., McGraw-Hill, N. Y.

Sentić, S., S. L. Sessions, and Ž. Fuchs (2015), Diagnosing DYNAMO convection with weak temperature gradient simulations, *J. Adv. Model. Earth Syst.*, *7*, 1849–1871, doi:10.1002/2015MS000531.

Sessions, S. L., S. Sugaya, D. J. Raymond, and A. H. Sobel (2010), Multiple equilibria in a cloud-resolving model using the weak temperature gradient approximation, *J. Geophys. Res.*, *115*, D12110, doi:10.1029/2009JD013376.

Sessions, S. L., M. J. Herman, and S. Sentić (2015), Convective response to changes in the thermodynamic environment in idealized weak temperature gradient simulations, *J. Adv. Model. Earth Syst.*, *7*, 712–738, doi:10.1002/2015MS000446.

Singh, M. S., and P. A. O'Gorman (2013), Influence of entrainment on the thermal stratification in simulations of radiative-convective equilibrium, *Geophys. Res. Lett.*, *40*, 4398–4403, doi:10.1002/grl.50796.

Sobel, A. H., and C. S. Bretherton (2000), Modeling tropical precipitation in a single column, *J. Clim.*, *13*, 4378–4392.

Sobel, A. H., G. Bellon, and J. Bacmeister (2007), Multiple equilibria in a single-column model of the tropical atmosphere, *Geophys. Res. Lett.*, *34*, L22804, doi:10.1029/007GL031320.

Sobel, A. H., E. D. Maloney, G. Bellon, and D. M. Frierson (2009), Surface fluxes and tropical intraseasonal variability, *J. Adv. Model. Earth Syst.*, *2*, 2, doi:10.3894/JAMES.2010.2.5.

Wang, S., and A. H. Sobel (2011), Response of convection to relative sea surface temperature: Cloud-resolving simulations in two and three dimensions, *J. Geophys. Res.*, *117*, D02112, doi:10.1029/2011JD016847.

Wang, S., and A. H. Sobel (2012), Impact of imposed drying on deep convection in a cloud-resolving model, *J. Geophys. Res.*, *117*, D02112, doi:10.1029/2011JD016847.

Wang, S., A. H. Sobel, and Z. Kuang (2013), Cloud-resolving simulation of TOGA-COARE using parameterized large-scale dynamics, *J. Geophys. Res. Atmos.*, *118*, 6290–6301, doi:10.1002/jgrd.50510.

Yano, J.-I., and K. Emanuel, (1991), An improved model of the equatorial troposphere and its coupling with the stratosphere, *J. Atmos. Sci.*, *48*, 377–389.